

STUDY ON THE QUANTITATIVE MODEL OF OIL SHALE POROSITY IN THE PYROLYSIS PROCESS BASED ON PYROLYSIS KINETICS

JIAN LIU^{(a,b)*}, WEIGUO LIANG^(a,b), ZHIQIN KANG^(b,c),
HAOJIE LIAN^(a,b), YIDE GENG^(a,b)

- ^(a) College of Mining Engineering, Taiyuan University of Technology, Taiyuan, Shanxi 030024, China
- ^(b) Key Lab of In-situ Property-improving Mining of Ministry of Education, Taiyuan, Shanxi 030024, China
- ^(c) Mining Technology Institute, Taiyuan University of Technology, Taiyuan, Shanxi 030024, China

Abstract. Investigation of the porosity variation of oil shale during the pyrolysis process is of great importance in understanding the migration mechanism of pyrolysis products. Using the Fushun oil shale of China as an example and taking into account the fact that the porosity change of oil shale arises from pyrolysis of kerogen at high temperature, in this paper, the thermal curve of oil shale was employed to obtain its pyrolysis rate equation. A quantitative model of oil shale porosity during pyrolysis was constructed. The porosity of oil shale under different pyrolysis conditions was determined using the conventional method, computed tomography (CT) and the mercury intrusion method. The calculated results were in good agreement with the experimental data.

Keywords: oil shale pyrolysis, porosity change mechanism, quantitative model, conventional method, computed tomography, mercury intrusion method.

1. Introduction

The pore structure of oil shale changes greatly in the process of pyrolysis. As one of the main migration channels for oil and gas, the porosity and permeability of oil shale have a significant influence on the migration of pyrolysis products. In recent years, some researchers have studied the porosity and permeability of oil shale after pyrolysis. For example, Kang [1] measured the porosity of oil shale in the Fushun West Opencast Mine under

* Corresponding author: e-mail 5102135@163.com

different temperature conditions using conventional methods. The results showed that the porosity of oil shale changed slightly from room temperature to 200 °C. After the temperature reached 200 °C and above, the porosity increased substantially with the increase of temperature [1]. Kang et al. [2] studied the internal fracture characteristics of oil shale under different temperature conditions using the micro computed tomography (CT) technique. The researchers found that the pore fissures produced by pyrolysis were the controlling factors of oil shale permeability. Esemé et al. [3] conducted high temperature triaxial compression tests on oil shales formed in different environments and geological periods. The results showed that the permeability of oil shale in the original state was low and further reduced after compression; however, with increasing temperature and output of oil and gas, the porosity gradually increased. Tiwari and Miller [4] studied the formation of inner pores before and after pyrolysis of Green River oil shale in the United States. It was revealed that a number of pore structures were formed in the oil shale after pyrolysis, and the permeability increased from 173 Darcy before pyrolysis to 2919 Darcy after pyrolysis. Zhao [5] measured the porosity of oil shale of the Fushun West Opencast Mine and Daqing Laoheishan of China at different temperatures. The porosity of oil shale increased with increasing temperature, and the relationship between the porosity and temperature of oil shale was obtained by statistical fitting. Jiang [6] measured the porosity of Chinese Fuyu oil shale before and after pyrolysis and concluded that the porosity increased at higher temperature: the respective values at room temperature, 300 °C and 500 °C were 2.5%, 10.1% and 19.1%. Qiu [7] found that the porosity and permeability of the oil shale layer increased significantly after pyrolysis, and the pores and fissures caused a hydraulic connection between the oil shale layer and its aquifers on the top and bottom. Then, the pollutants generated in the process of pyrolysis moved into the adjacent aquifers and caused groundwater pollution. Bai and Guo [8] investigated the formation and evolution of the pore structure of Chinese Huadian oil shale at 100–800 °C. The results showed that the temperature could significantly affect the evolution of the pore structure. The oil shale porosity and permeability increased with increasing temperature, and the escape of pyrolysis products would increase the porosity [8]. Based on the above, a conclusion can be drawn that the temperature can greatly affect the porosity and permeability of oil shale, both of which increase gradually with increasing temperature. However, the current research is mainly restricted to the comparison between the oil shale porosity before and after pyrolysis, lacking an understanding of its continuous variation throughout the pyrolysis process. The main reason is that in the experiments it is very difficult to terminate oil shale pyrolysis immediately and observe porosity in real time. Thus, the qualitative models in the above-mentioned work [5] are mainly based on statistical fitting. Few researchers have analysed and established the mathematical model of oil shale porosity in the pyrolysis process from the perspective of the mechanical mechanism.

To fill the research gap, this paper quantitatively studied the change of oil shale porosity during the pyrolysis process based on pyrolysis kinetics, which is of great practical significance to studies of the migration law and numerical simulation of pyrolysis products.

2. Materials and methods

2.1 Oil shale samples

The oil shale in this study was taken from the Fushun West Opencast Mine, Liaoning Province, China. The samples had dark brown colour and oil luster, and cracks were not developed. According to the experimental requirements, the oil shale samples were processed into powder (grain size ≤ 0.2 mm), cubic specimen (the length approximately 4–5 cm), and cylindrical specimen ($\Phi 3.8 \times 15$ mm).

2.2. Experimental procedure

The porosity data used in this study come from previous studies [1, 5]. For the sake of explanation, the experimental scheme is briefly described below.

2.2.1. Thermogravimetry experiment on oil shale

First, the DTU-2B thermogravimetric analyser (Beijing Boyuan Precision Technology Development Co., Ltd., China) was opened, and high purity nitrogen was let flow in as the carrier gas. The heating rate was set at 30 °C/min and the final temperature at 950 °C, the mass of the crucible was cleaned. Then, the oil shale powder (grain size ≤ 0.2 mm), which came from the Fushun West Opencast Mine, was put into the crucible, and the mass of the powder was determined (168.63 mg). Finally, the heating furnace was started to measure the change in the mass of the oil shale powder with the increase in temperature [1].

2.2.2. Oil shale porosity test after pyrolysis

For conducting the test of oil shale porosity after pyrolysis, the conventional method [1], computed tomography [5] and the mercury intrusion method [5] were used.

2.2.2.1. Conventional method

Based on Chinese national standards for determination of the physical properties of coal and rock (MT40-80 [9], GB217-81 [10], MT41-80 [11]), the cubic specimens with a length of approximately 4–5 cm were wrapped in thin aluminium foil (melting point 680 °C) and placed in the oven. Then the oil shale porosity at temperatures of 20, 100, 200, 300, 400, 500, and 600 °C, each being held constant for 60 min, was calculated by measuring the specific gravity and bulk density of oil shale at the same temperatures.

2.2.2.2. Computed tomography

In performing computed tomography, the oil shale cylindrical specimens ($\Phi 3.8 \times 15$ mm) were heated in the muffle furnace. The target temperature was 400 °C, 500 °C and 600 °C. After the temperature was raised to the target temperature, the specimens were heated for 30 min, the furnace was then turned off, and the specimens spontaneously cooled down to room temperature.

Then a cooled specimen was fixed on the CT scanning table, the scanning parameters were adjusted, the scanning was started and CT greyscale images were obtained.

By using the CT image analysis system, the three-dimensional reconstruction of oil shale specimens was performed, and the digital model composed of the pore and solid skeleton was obtained. Based on this model, the porosity could be calculated using pore volume statistics.

2.2.2.3. Mercury intrusion method

The cylindrical specimens ($\Phi 3.8 \times 15$ mm) at different temperatures (20, 300, 400, 450, 500 °C, each temperature being kept constant for 30 or 60 min) were placed in the Pore Master 33 mercury injection apparatus, which was sealed and evacuated. Then the low pressure test (1.5–350 kPa) was carried out. After that, the specimens were put into the high pressure warehouse for the high pressure test (140–231 MPa).

Based on the amount of mercury entering the pore system under different pressures, the pore size and pore distribution were calculated, and the porosity was obtained.

2.3. Methods

2.3.1. Model of oil shale porosity

Kerogen is the main form of organic matter in oil shale. The pyrolysis of oil shale represents the pyrolysis of kerogen. In the process of oil shale pyrolysis, kerogen is pyrolysed into shale oil, pyrolysis gas and other products. With the precipitation of pyrolysis products, oil shale gradually becomes porous. The precipitation would make the porosity of oil shale change. Based on the above analysis, the porosity of oil shale increases as a result of the pyrolysis of kerogen.

The porosity of oil shale during pyrolysis can be calculated by Equation (1):

$$n' = n + \Delta n = n + \frac{m \cdot \alpha / \rho_o - m_c \cdot \alpha / \rho_c}{M / \rho_s} \times 100\% = n + \frac{p_o \cdot \alpha \cdot \rho_s}{\rho_o} - \frac{p_c \cdot \alpha \cdot \rho_s}{\rho_c}, \quad (1)$$

where M is the mass of oil shale, m is the mass of kerogen, m_c is the mass of the carbon residue, ρ_s is the density of oil shale, ρ_o is the density of

kerogen, ρ_c is the density of the carbon residue, the kerogen content in oil shale is $p_o = \frac{m}{M} \times 100\%$, the residual carbon content in oil shale is $p_c = \frac{m_c}{M} \times 100\%$, n is the porosity of oil shale before pyrolysis, n' is the porosity of oil shale after pyrolysis, Δn is the change in oil shale porosity during pyrolysis, and α is the conversion ratio of kerogen. Of the above parameters, n can be determined by the experiment, α can be obtained from the pyrolysis reaction rate equation, and ρ_s , ρ_o , ρ_c , p_o and p_c can be obtained directly or indirectly from the relevant data.

2.3.2. Method for establishing the rate equation for oil shale pyrolysis

In this paper, the kinetic analysis of the mass-temperature curves of oil shale pyrolysis was carried out using the Coats-Redfern (C-R) method [12–16]. The kinetic equation is expressed as follows:

$$\ln \left[\frac{1 - (1 - \alpha)^{1-n}}{T^2(1-n)} \right] = \ln \left[\frac{AR}{\beta D} \left(1 - \frac{2RT}{D} \right) \right] - \frac{D}{RT} \quad (n \neq 1), \quad (2)$$

$$\ln \left[\frac{-\ln(1-\alpha)}{T^2} \right] = \ln \left[\frac{AR}{\beta D} \left(1 - \frac{2RT}{D} \right) \right] - \frac{D}{RT} \quad (n=1). \quad (3)$$

For most of the pyrolysis reaction temperatures and D values, $D/Rt \gg 1$, so $(1 - 2RT/D) = 1$, and the first term at the right end of Equations (2) and (3) can be considered a constant. When $n \neq 1$, a linear fitting of $\ln \left[\frac{1 - (1 - \alpha)^{1-n}}{T^2(1-n)} \right]$ and $\frac{1}{T}$ can be done. When $n=1$, a linear fitting of $\ln \left[\frac{-\ln(1-\alpha)}{T^2} \right]$ and $\frac{1}{T}$ can be done. From the intercept $\ln \left(\frac{AR}{\beta D} \right)$ and slope $-\frac{D}{R}$ of the fitted line, the frequency factor A and the activation energy D can be calculated, and then, the pyrolysis rate constant k of oil shale at any temperature T can be found using Equation (4):

$$k = A \cdot e^{-D/RT}. \quad (4)$$

Then, the pyrolysis reaction rate equation for oil shale at any temperature T can be obtained as follows:

$$\frac{d\alpha}{dt} = k \cdot (1 - \alpha)^n. \quad (5)$$

Many studies have shown that the oil shale pyrolysis can be described as a first-order reaction [12–15, 17–19]; so Equation (5) can be written as follows:

$$\frac{d\alpha}{dt} = k \cdot (1 - \alpha). \quad (6)$$

Next, by integration of Equation (6), the functional relationship between the conversion ratio of kerogen and the time under constant temperature conditions can be obtained as follows:

$$\alpha = 1 - e^{-kt}. \quad (7)$$

In the above equations, $\frac{d\alpha}{dt}$ is the reaction speed, percent/min; k is the rate constant; t is the time; n is the reaction order; A is the frequency factor, min^{-1} ; D is the activation energy, kJ/mol; R is the gas constant (its value is 8.314 J/(mol·K)); T is the absolute temperature, K; α is the conversion ratio of kerogen at temperature T (its equation is $\alpha = \frac{w_0 - w_T}{w_0 - w_\infty}$, where w_0 is the initial mass of the oil shale sample, w_T is the sample mass at temperature T , and w_∞ is the mass of the residue when the pyrolysis reaction is terminated), and β is the heating rate, °C/min.

3. Results and discussion

3.1. Results

3.1.1. Analysis of thermogravimetry experiment on oil shale

Figure 1 shows the TG curve (the curve of the relationship between the oil shale mass and temperature) and the DTG curve (the curve of the relationship between the oil shale mass change rate and temperature) of oil shale. Clearly, the weight loss of oil shale underwent three different stages.

In the first stage, from room temperature to 300 °C, there appeared a small decline in the DG curve. At the same time, the first concave peak appeared in the DTG curve. The weight loss accounted for 2.24% of the sample mass, mainly caused by the precipitation of water (structural water, interlayer water, etc.) in oil shale.

In the second stage, from 300 to 600 °C, the TG curve made a quick and sharp fall, and the maximum concave peak appeared in the DTG curve. The weight loss of oil shale was huge, accounting for 16.21% of its sample mass. The pyrolysis of kerogen in oil shale, which resulted in the formation of shale oil and gaseous products, is the main reason for the weight loss in this stage.

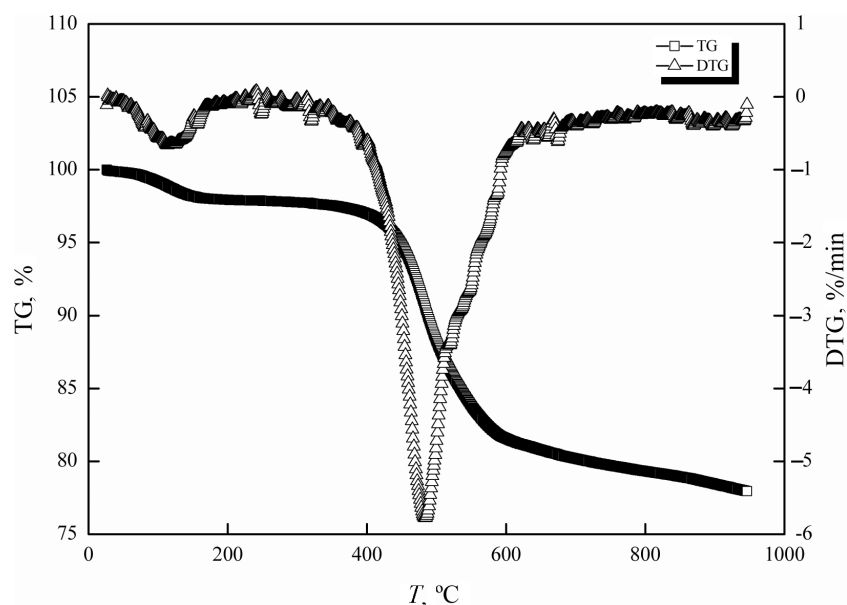


Fig. 1. Pyrolysis TG and DTG curves of oil shale in the Fushun West Opencast Mine.

In the third stage, above 600 °C, the TG curve continued to decline. The change in the DTG curve was relatively stable and not obvious, and the weight loss was 3.59% of the oil shale sample mass. The thermal decomposition of carbonates in oil shale is generally believed to occur in this stage, as is the high-temperature carbonization of the fixed carbon in which a small amount of gas is generated. All of these processes resulted in a certain weight loss.

Therefore, the pyrolysis of oil shale occurred mainly in the temperature range of 300–600 °C [1].

3.1.2. Variation in oil shale porosity

The variation in the porosity of oil shale at 100–600 °C is presented in Table 1. It was not difficult to discover that with increasing temperature, the porosity of oil shale continued to rise, especially in the temperature region of 300–500 °C where the porosity increased significantly. When the temperature rose to 600 °C, the porosity changed but a little. This finding was similar to the result obtained previously by Zhao [5]. Zhao studied the physical and mechanical properties of oil shale from the Fushun West Opencast Mine at different temperatures and found that the elastic modulus and compressive strength of oil shale decreased considerably in the temperature range of 300–500 °C, but at 600 °C, the elastic modulus increased and the compressive strength decreased. The change of the compressive strength was not significant, probably due to the pyrolysis of the fixed

carbon at given temperatures [5]. The pyrolysis of kerogen occurred mainly at 300–500 °C, while from 500 to 600 °C, the fixed carbon and other substances were pyrolysed. Based on the above analysis, in this paper, the temperature range of oil shale pyrolysis was determined to be 300–500 °C.

Table 1. Porosity of oil shale samples at different temperatures

Temperature, °C	Porosity measured by the conventional method [1], %	Porosity measured by the mercury intrusion method [5], %	Porosity measured by CT [5], %
20	2.14	1.71	1.77
100	3.33	–	–
200	4.56	–	–
300	7.34	–	–
400	18.80	20.33	24.14
450	–	23.41	–
500	25.50	29.76	33.71
600	26.40	31.29	36.07

Note: “–” represents no data.

3.1.3. Establishment of the pyrolysis reaction rate equation for oil shale

According to the research method described in Section 2.2.2 and the data from the thermogravimetric curve of oil shale, the linear fitting result of $\ln\left[\frac{-\ln(1-\alpha)}{T^2}\right]$ and $\frac{1}{T}$ in the pyrolysis stage at 300–500 °C is shown in Figure 2.

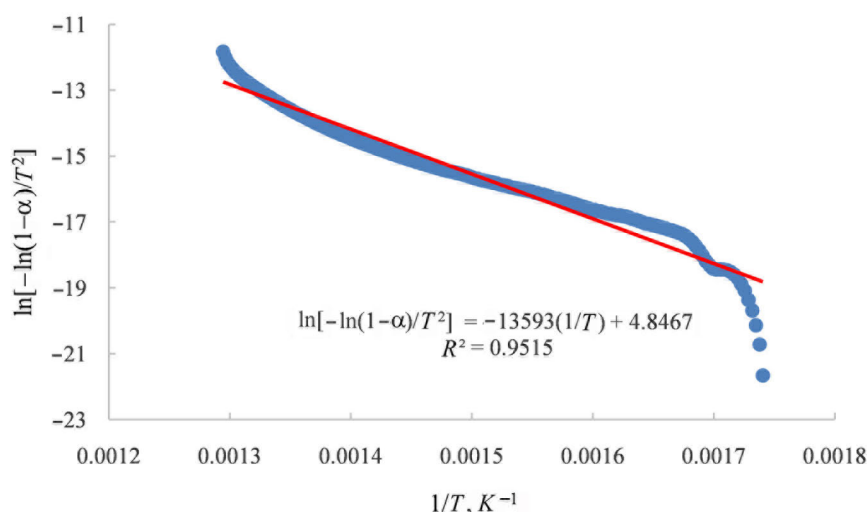


Fig. 2. Linear fitting of $\ln[-\ln(1-\alpha)/T^2]$ and $1/T$.

In this work, the activation energy D was 113 kJ/mol, and the frequency factor A was $5.2 \times 10^7 \text{ min}^{-1}$. Then, the pyrolysis reaction rate equation for oil shale at different temperatures could be obtained.

The pyrolysis reaction rate equation for oil shale at 400 °C could be expressed as follows:

$$\alpha = 1 - e^{-kt} = 1 - e^{-8.92 \times 10^{-2} \cdot t} \quad (8)$$

The pyrolysis reaction rate equation for oil shale at 450 °C could be given as follows:

$$\alpha = 1 - e^{-kt} = 1 - e^{-0.36 \cdot t} \quad (9)$$

The pyrolysis reaction rate equation for oil shale at 500 °C could be written as follows:

$$\alpha = 1 - e^{-kt} = 1 - e^{-1.21 \cdot t} \quad (10)$$

The time required for the completion of oil shale pyrolysis (kerogen conversion ratio was calculated to be 0.99) at different temperatures is given in Table 2.

From Table 2 it is seen that the time required for the completion of oil shale pyrolysis decreased rapidly with increasing temperature. Nearly one hour was required at 400 °C to complete the pyrolysis process, while at 450 °C and 500 °C, it could be completed within more than ten minutes, or even within a few minutes. These results were consistent with those of previous researches [12, 14].

Table 2. Time required for the completion of oil shale pyrolysis at different temperatures

Temperature, °C	Conversion ratio, %	Time, min
400	99	51.63
450	99	12.80
500	99	3.80

3.1.4. Quantitative calculation of oil shale porosity

3.1.4.1. Values of parameters

According to literature data, the density of Fushun oil shale is 1.9–2.2 g/cm³, the organic matter content is 18.7–19.1%, and the organic matter content minus the asphalt content is the kerogen content [20]. The asphalt content in the oil shale is low, being generally less than 1%. The density of the carbon residue is 1.8–2.1 g/cm³. In addition, from the aluminium retort analysis, shale oil accounts for 6.7% of the oil shale mass, and gas accounts for 3.3%. The Fushun oil shale pyrolysis process model (Eq. (2)) shows that the kerogen is first depolymerized into asphalt, and the kinetic equation obtained

from the thermogravimetric data actually describes the process of pyrolysis of asphalt into oil shale, gas and carbon residue asphalt [12]. Since the asphalt in the organic matter is also pyrolysed, in this paper, to study the change in oil shale porosity during pyrolysis, the kerogen was substituted by organic matter. In addition, as is known from Section 3.1.1., the pyrolysis of oil shale began at a temperature of 300 °C. To eliminate the influence of moisture on porosity, before pyrolysis the porosity at 200 °C was selected as its base value, and the porosity of oil shale during the pyrolysis process was then calculated at 300 °C, 400 °C and 500 °C.

The values of parameters n , p_c and p_s used in this work were from [20] and ρ_o was from [21], and were as follows:

$$n = 4.56\%, \quad (11)$$

$$\rho_c = \frac{1.8 + 2.1}{2} = 1.95 \text{ g/cm}^3, \quad (12)$$

$$\rho_s = \frac{1.9 + 2.2}{2} = 2.05 \text{ g/cm}^3, \quad (13)$$

$$\rho_o = 1.104 \text{ g/cm}^3, \quad (14)$$

$$p_o = \frac{18.7\% + 19.1\%}{2} = 18.9\%, \quad (15)$$

$$p_c = 18.9\% - 6.69\% - 3.30\% = 8.91\%. \quad (16)$$

3.1.4.2. Calculation of the porosity of oil shale during pyrolysis

Using the above method (see 2.3.), the oil shale porosity at different pyrolysis temperatures and times was calculated; the results are shown in Figure 3 and presented in Table 3.

From Figure 3 it can be seen that the oil shale porosity increased with increase in temperature from 400 to 500 °C. At 400 °C, the porosity increased relatively slowly, but at 450 °C and 500 °C, in the initial stage of pyrolysis, it increased very rapidly and then the growth rate slowed. Compared with oil shale porosity at 200 °C when there was no marked

Table 3. Oil shale porosity under different pyrolysis conditions

Time, min	Porosity at 400 °C, %	Porosity at 450 °C, %	Porosity at 500 °C, %
5	13.82	26.03	30.23
10	19.74	29.58	30.29
30	28.52	30.29	30.29
60	30.17	30.29	30.29

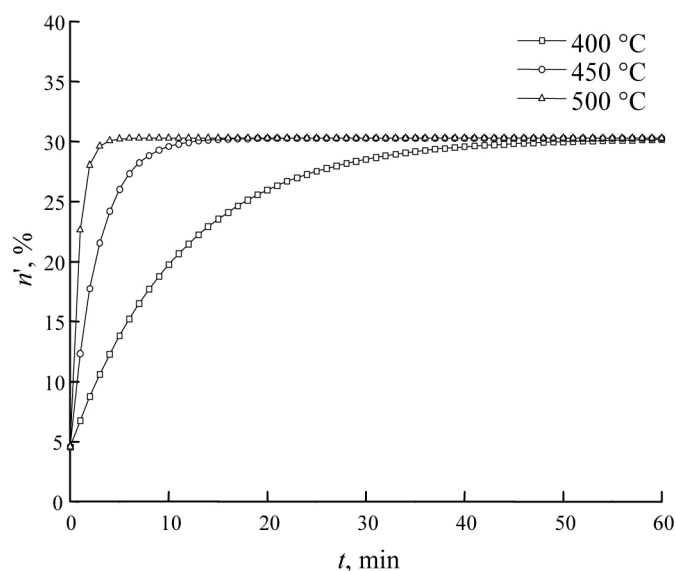


Fig. 3. Porosity of oil shale during pyrolysis.

change in it, after a 10-minute pyrolysis, at 400 °C, the porosity increased little, by approximately 15% only, and at 450 °C, by ca 25%; at 500 °C, the porosity increased most, by about 26%.

3.2. Verification

The porosity of oil shale was calculated at 400 °C, 450 °C and 500 °C during a certain period of time and the values were compared with the experimental data obtained under the same temperature conditions. The results are given in Table 4.

Table 4. Comparison between the calculated and measured values of porosity

Temperature, °C	Time, min	Calculated value, %	Measured value [1, 5], %			Absolute error, %		
			Conventional method	Mercury intrusion method	CT	Conventional method	Mercury intrusion method	CT
400	30	28.52	–	20.33	24.14	–	8.19	4.38
	60	30.17	18.80	–	–	11.37	–	–
450	30	30.29	–	23.41	–	–	6.88	–
	60	30.29	–	22.65	–	–	7.64	–
500	30	30.29	–	29.76	33.71	–	0.53	3.42
	60	30.29	25.50	–	–	4.79	–	–

Note: “–” represents no data.

3.2.1. Verification with the results of the conventional method

The pyrolysis time of the oil shale specimen was 60 min. By this time, the theoretical oil shale conversion ratios at 400 °C and 500 °C had exceeded 99%. Compared with the conventional method, the calculated porosity was higher. The absolute error of porosity at 500 °C was small, only 4.8%, while at 400 °C it was the largest, 11.4%, which was caused by the effect of the oil shale sample size on the results. Although the oil shale sample was in a high-temperature environment, heat transfer and temperature rise could not take place simultaneously. It took a certain amount of time before the temperature distribution within the sample became uniform. The larger the sample size, the higher the temperature and the longer the time required for heat transfer. The pyrolysis rate equation in this paper was based on the pyrolysis weight loss data about ground oil shale samples (particle size ≤ 0.2 mm). There was a big difference in particle size between the sample used for porosity calculations and the kinetic sample. Earlier research has shown that at a temperature of 475 °C, 30–40 min was needed for the transfer of heat for the oil shale sample with a size of 40–70 mm [20]. At 400 °C, a longer time was required to keep the temperature constant. At this temperature, the oil shale conversion ratio of 99% was achieved in 51.6 min. A longer heat transfer time greatly affected the oil shale conversion ratio, so the absolute error of porosity at 400 °C was large. At 500 °C, only 3.8 min was needed to obtain the 99% conversion ratio. Although the heat transfer time was further extended over 60 min, there was still enough pyrolysis time to minimize the difference between the actual and theoretical conversion ratios, so the absolute error of oil shale porosity at 500 °C was also small. In addition, the thin aluminium foil the oil shale specimen was wrapped in hindered the precipitation of the pyrolysis products, as a result of which these were partly detained in the specimen, which considerably decreased the measured porosity.

3.2.2. Verification with the results of the mercury intrusion method

Compared with the conventional method, the size of the specimen measured by the CT method was small, no wrapping in thin aluminium foil was made. The theoretical conversion ratio at 400 °C was approximately 93%, and the conversion rate at 450 °C and 500 °C had exceeded 99%. Similarly, based on the sample size effect, the theoretical porosity value was still larger than the one measured by the CT method. Although the specimen size was small, a certain amount of heat transfer time was still needed, so the actual conversion ratio was still lower than the theoretical one. The absolute error of porosity was still large, but due to the reduction of the heat transfer time, it was reduced from about 11.4 to 8.2%. Similarly, the heat transfer time was shortened and the conversion ratio reached 99% just in 3.8 min, while the absolute error of porosity after 30 and 60 min was approximately 6.9 and 7.6%, respectively. At 500 °C, after 3.8 min, the conversion ratio reached

99%, so the absolute error of oil shale porosity was very small, 0.53%. As the mercury intrusion method can measure only the porosity of opening pores, the measured porosity value was generally small.

3.2.3. Verification with the results of the CT method

In CT tests, similar-sized oil shale samples and similar pyrolysis conditions were used as in the mercury intrusion test. As seen from Table 4, the difference between the theoretical porosity value and the CT measured value is small, its absolute errors at 400 °C and 500 °C are about 4.4% and 3.4%, respectively. The porosity value measured at 500 °C is slightly larger than the calculated one, which may be accounted for by the difference in sample size. In this paper, the calculated values of relevant parameters were the average figures. Considering that the mercury intrusion method can measure the porosity of opening pores only, while CT can determine the porosity of all pores, the latter method provided more accurate results, yet the difference in porosity values between the two approaches was small. This also proved the accuracy of the quantitative model for the porosity measurement of oil shale during the pyrolysis process.

In summary, although the oil shale sample size influenced the porosity results, the quantitative model established on the basis of the pyrolysis reaction kinetics could still accurately calculate the porosity of oil shale during pyrolysis, and the error was small. The use of a small-sized specimen during a long pyrolysis time is especially suited for this model.

3.3 Discussion

To simulate the change of porosity in the oil shale pyrolysis process accurately, it is necessary to establish the heat transfer equation based on the thermal equilibrium equation, combined with the thermal diffusion coefficient, specific heat capacity and thermal conduction coefficient of a large block of oil shale. Therefore, the temperature distribution within and the change of porosity of oil shale are established, and then, the porosity model can be modified and improved by combining it with the pyrolysis kinetic equation. Only in this way can the quantitative calculation of the porosity of lump oil shale in the pyrolysis process be realized. The time required for the temperature of a large block of oil shale to become uniform is proportional to the square of the block size [22, 23], which can provide a theoretical basis for further corrections to our model.

From the point of view of the pyrolysis rate, 400–500 °C is the most optimum range of temperature for oil shale pyrolysis. However, a high temperature may cause the porosity of oil shale to increase sharply in a short time. For example, the porosity of Fushun West Opencast Mine oil shale reached 30.29% in tens of minutes in theory. The increase in temperature is likely to make oil shale change from the water-resisting layer to the permeable one. When it comes to the in situ pyrolysis mining area, then, as a result

of temperature rise, there is a strong possibility that waste contaminants generated in the oil shale pyrolysis will get into the aquifer and pollute groundwater. Therefore, the excessive pursuit of an increased pyrolysis rate is not desirable. The optimum pyrolysis temperature should be selected by considering the production efficiency, injection cost, environmental impacts, etc. Of course, the in situ porosity is also related to confining pressure. In the current study, the change of porosity under pressure conditions is not considered. This should be related to the elastic modulus of oil shale pyrolysis, which needs to be discussed in a future study.

4. Conclusions

1. Taking Fushun oil shale as an example, on the basis of the pyrolysis kinetics of oil shale, a quantitative model of its porosity during the pyrolysis process was established. The calculated results showed that the growth rate of porosity increased with the rise of temperature.
2. The porosity of the Fushun oil shale specimen at 400 °C, 450 °C and 500 °C during 30 and 60 min was determined using the conventional method, computed tomography and the mercury intrusion method. The calculated values of the model were in good agreement with the experimental results. The porosity of oil shale during pyrolysis could be calculated accurately by using this model.
3. Although the method employing the pyrolysis reaction kinetics is feasible for calculating the porosity of oil shale during pyrolysis, the effect of sample size on the results should be taken into account. In this paper, the research object was a small-sized oil shale specimen, so the temperature within it became uniform during a short time. At the same time, the distribution of temperature in lump oil shale is unlikely to become uniform in a short time. Therefore, the internal heat conduction process of lump oil shale has become the key controlling process for its own pyrolysis. Construction of a quantitative model of the porosity change of lump oil shale will be a subject of a future research.

Acknowledgment

This work was supported by the National Natural Science Foundation of China (Grant No. 51604182).

REFERENCES

1. Kang, Z. *The Pyrolysis Characteristics and In-situ Hot Drive Simulation Research that Exploit Oil-gas of Oil Shale*. PhD thesis, Taiyuan University of Technology, 2008 (in Chinese with English abstract).

2. Kang, Z., Yang, D., Zhao, Y., Hu, Y. Thermal cracking and corresponding permeability of Fushun oil shale. *Oil Shale*, 2011, **28**(2), 273–283.
3. Esemé, E., Krooss, B. M., Littke, R. Evolution of petrophysical properties of oil shales during high-temperature compaction tests: Implications for petroleum expulsion. *Mar. Petrol. Geol.*, 2012, **31**(1), 110–124.
4. Tiwari, P., Miller, J. D. Characterization of oil shale pore structure before and after pyrolysis by using X-ray micro CT. *Fuel*, 2013, **107**, 547–554.
5. Zhao, J. *Experimental Study on the Microscopic Characteristics and Mechanical Property of Oil Shale under High Temperature & Three-Dimensional Stress*. PhD thesis, Taiyuan University of Technology, 2014 (in Chinese with English abstract).
6. Jiang, X. *Study about the Impacts of Oil Shale In-situ Mining on Groundwater Environment*. PhD thesis, Jilin University, 2014 (in Chinese with English abstract).
7. Qiu, S. *Experimental Study on the Impacts of Oil Shale In-situ Pyrolysis on Groundwater Hydrochemical Characteristics*. PhD thesis, Jilin University, 2016 (in Chinese with English abstract).
8. Bai, F., Guo, M. Evaluation of the porous structure of Huadian oil shale during pyrolysis using multiple approaches. *Fuel*, 2017, **187**, 1–8.
9. The Ministry of Coal Industry of People's Republic of China. *MT 40-80, Rock Apparent Density Testing Standard*. China Standards Press, Beijing, 1980 (in Chinese).
10. The Ministry of Coal Industry of People's Republic of China. *GB 217-81, Coal True Relative Density Testing Standard*. China Standards Press, Beijing, 1981 (in Chinese).
11. The Ministry of Coal Industry of People's Republic of China. *MT 41-80, Rock Porosity Testing Standard*. China Standards Press, Beijing, 1980 (in Chinese).
12. Guo, S., Geng, L. Study on pyrolysis kinetics of oil shales by thermogravimetry. *J. Fuel. Chem. & Tech.*, 1986, **14**(3), 21–27 (in Chinese with English abstract).
13. Wang, G. *Study on Kinetics of Oil Shale Pyrolysis Products Generation Process*. Master thesis, Northeast Dianli University, 2012 (in Chinese with English abstract).
14. Geng, L., Guo, S. The kinetics of the thermal decomposition of Huadian oil shale by thermogravimetry. *J. Dalian. Univ. Tech.*, 1984, **23**(4), 39–44 (in Chinese with English abstract).
15. Yang, J. Thermogravimetric investigation of Maoming oil shale pyrolysis kinetics. *J. China. Univ. Petrol. (Edition of Natural Science)*, 1982, (3), 85–93 (in Chinese with English abstract).
16. Coats, A. W., Redfern, J. P. Kinetic parameters from thermogravimetric data. *Nature*, 1964, **201**, 68–69.
17. Weitkamp, A. W., Gutberlet, L. C. Application of a microretort to problems in shale pyrolysis. *Ind. Eng. Chem. Proc. Des. Dev.*, 1970, **9**(3), 386–395.
18. Shih, S. M., Sohn, H. Y. Nonisothermal determination of the intrinsic kinetics of oil generation from oil shale. *Ind. Eng. Chem. Proc. Des. Dev.*, 1980, **19**(3), 420–426.
19. Braun, R. L., Rothman, A. J. Oil-shale pyrolysis: Kinetics and mechanism of oil production. *Fuel*, 1975, **54**(2), 129–131.
20. Qian, J., Yin, L. *Oil Shale: Petroleum Alternative*. China Petrochemical Press, Beijing, 2008 (in Chinese).

21. Qin, K. Investigation on the constitution and structure of Maoming and Fushun oil shale. Part 3: Average building block of organic matter. *J. Fuel. Chem & Tech.*, 1986, **14**(1), 3–10 (in Chinese with English abstract).
22. Li, S., Qian, J. Study of the pyrolysis of Maoming oil shale lumps. *Fuel*, 1991, **70**(12), 1371–1375.
23. Li, S., Qian, J. Investigation on the pyrolysis of Fushun oil shale and Estonian Kukersite lumps. *Oil Shale*, 1992, **9**(3), 222–230.

Presented by S. Li

Received July 3, 2017